

FIG. 1. Comparison of τ/τ_B vs $\pi^2(C^2aq^2\mathcal{L}^2S^2)^{-1}$; τ/τ_B represents the experimentally reported volumes, and a , q , \mathcal{L} , and S are estimates taken from experimental papers.

This theory is by no means complete. However, it is hoped that future experiments (in particular, fluctuation measurements in Tokamaks) will determine whether this theory is correct. Incidentally, the convective cell loss is also covered by the present theory in view of the fact that our theory does not have any time dependence.

Finally, for Tokamak plasmas the diffusion coefficient of Eq. (18) can be expressed as

$$D = 4C^2K^2D_{clp}, \tag{22}$$

where C is 3 for the best fit with $K = 2$, and

$$D_{clp} = \frac{mv_C}{e^2B_p^2} (kT_e + kT_i)$$

if $T_i \neq 0$; that is, D_{clp} is the classical diffusion coefficient with the poloidal field only.

*Work performed under the auspices of the U. S. Atomic Energy Commission, Contract No. AT(30-1)-1238.

¹See, for example, L. A. Artsimovich, A. M. Anashin, E. P. Gorkunov, D. P. Ivanov, M. P. Petrov, and V. S. Strelkov, *Pis'ma Zh. Eksp. Teor. Fiz.* **10**, 130 (1969) [*JETP Lett.* **10**, 82 (1969)].

²See, for example, E. Hinov and A. S. Bishop, *Phys. Fluids* **9**, 195 (1966).

³See, for example, D. C. Robinson and R. E. King, in *Proceedings of the Third International Conference on Plasma Physics and Controlled Nuclear Fusion Research* (International Atomic Energy Agency, Vienna, Austria, 1969), Vol. I, p. 263.

⁴K. M. Young, *Phys. Fluids* **12**, 213 (1967).

⁵S. Yoshikawa, to be published.

⁶S. Yoshikawa and D. J. Rose, *Phys. Fluids* **5**, 334 (1962).

CONTROLLED PINNING IN SUPERCONDUCTING FOILS BY SURFACE MICROGROOVES*

D. D. Morrison and R. M. Rose

Department of Metallurgy and Materials Science and Center for Materials Science and Engineering, Massachusetts Institute of Technology, Cambridge, Massachusetts 02139

(Received 12 June 1970)

To test the idea that surface irregularities can pin fluxons, regular parallel microgrooves were created in the surfaces of homogeneous cast In-2% Bi foils by pressing diffraction gratings into the foils. The pinning force thus induced was zero for flux flow parallel to the grooves and a maximum for perpendicular flux flow; a very simple dependence on the spacing and strength of the pinners was found.

The surface contribution to pinning and flux flow in various Type II superconductors has been well documented.¹⁻⁴ It has been suggested⁵ that such effects may in some cases be very strong bulk pinning near the surface, and not a fundamental surface effect. For abraded surfaces,

this suggestion has been confirmed.⁶

We now wish to demonstrate that pinning also results from surface geometry, the precise control of which affords a technique for controlling both the spacing and strength of pinning centers. Pinning due to surface irregularities can explain

the differing observations of Swartz and Hart¹ and Joiner and Kuhl⁷ on the occurrence of the "peak and dip effect" in thin type-II Pb-Tl foils. The latter effect was attributed to the supercon-

ducting surface sheath, since the peak could be removed by copper electroplating.¹ We have duplicated these results, but we have also removed the J_c peak by plating only one side of the foil, contradicting the above conclusion. Copper plating removes the surface sheath from only one side; therefore the J_c peak should still be visible.

The abrasion of In-2% Bi alloys (Type II) produces grooving of the surface as well as cold work, as Fig. 1(a) shows. To eliminate the effects of cold work of any kind, In-2% Bi foils of 0.005 in. thickness were carefully cast and cooled between Pyrex plates. Grooves of the appropriate size were made by pressing diffraction gratings into one side of the foils. The casting-cooling-pressing sequence was critical. A typical result is shown in Fig. 1(b), and a schematic in Fig. 1(c). The pinning or the reduction in fluxon self-energy is (neglecting surface sheath and fluxon "spreading" effects at the surface) roughly that of an internal void of the same size and shape. In Fig. 2 we show typical J_c vs H_{\perp} data for current flow parallel and perpendicular to the grooves, with H always normal to the foil surface, illustrating the expected pinning anisotropy.

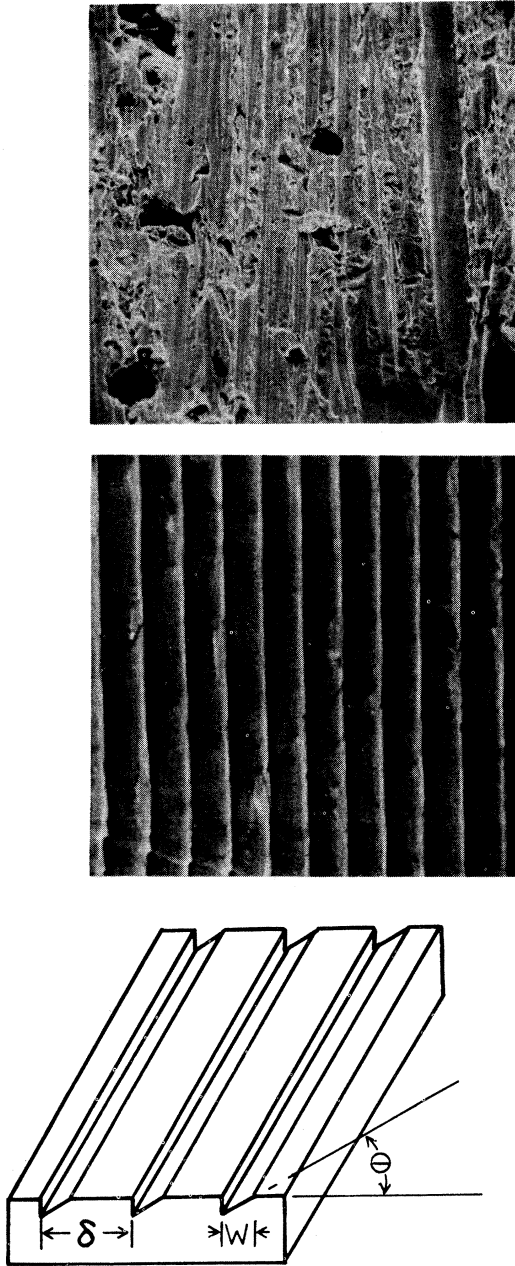


FIG. 1. (a) The surface of In-2% Bi foil abraded with No. 600 paper (scanning electron microscope, 490 \times). (b) In-2% Bi foil imprinted with diffraction grating, 590 lines/mm. (Scanning electron microscope, 5000 \times ; for the measurement of groove width, 20 000 \times was used when necessary.) (c) Schematic of imprinted surface, showing groove width w , blaze angle θ , and groove spacing δ .

A

B

C

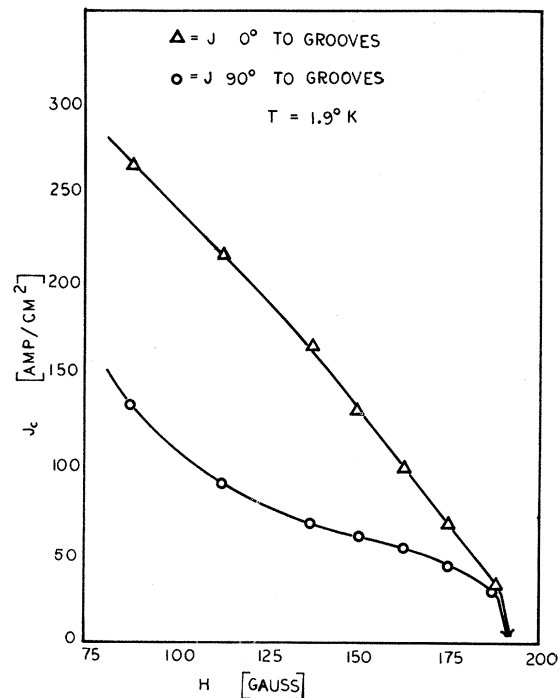


FIG. 2. J_c ($1 \mu V/cm$) vs H_{\perp} of In-2% Bi foil; H normal to the foil, current flow parallel and perpendicular to the grooves, which were spaced at 40 grooves per mm and were 6.25μ wide. The data for J perpendicular to the grooves are identical to those of the ungrooved foil, and represent "background."

If one considers only the effects of the grooves, there will be no pinning force when the flux lines are subjected to a Lorentz force in a direction parallel to the grooves. In fact, the curve in Fig. 2 for perpendicular current flow (i.e., flux flow parallel to the grooves) is identical to the data for ungrooved foils. Apparently the cold work which does occur during imprinting has too small an effect to be measured. We have done such experiments using gratings with spacings ranging from 12 to 1200 grooves/mm, and measured with the scanning electron microscope the size and spacing of the grooves. We find that, using various resistive criteria (e.g., $1 \mu\text{V}/\text{cm}$, $6 \mu\text{V}/\text{cm}$, extrapolation of the flux flow curve to $0 \mu\text{V}/\text{cm}$, etc.), that the critical Lorentz force is, within 2.4%, given by

$$\alpha_c = \text{const}[\Delta G(H)w \tan\theta/\delta] \quad (1)$$

per unit length of specimen, where $\Delta G(H)$ applies to the mixed-state-normal-state transition and the other symbols are explained in Fig. 1(c). The relation holds for groove widths w down to 0.27μ , or 2.4ξ . The next smallest sizes tested were the narrowest available to us; they were 0.13μ or about 1.2ξ wide and were totally ineffective as fluxon pinners, confirming the notion that the lower limit on the size of an effective pinner is of the order of the range of coherency. For reduced fields $0.65 < h < 1$ the critical pinning force decreased linearly, i.e., $\Delta G \cong \Delta G_0(1-h)$, which is consistent with the fact that our pinners are simple and have no superconducting properties of their own.

Because Eq. (1) applies to the initiation of flux flow or any arbitrary flux-flow rate in the linear region, we conclude that the static pinning force must be identified with (or at least proportional to) the dynamic pinning force commonly used in force balances with the viscous resistance and the Lorentz force, i.e.,

$$f_p(\text{dynamic}) = f_L - \eta V_\phi = f_p(\text{static}). \quad (2)$$

Notice that $f_p(\text{dynamic})$ is not proportional to $f_p^2(\text{static})$, as suggested by Yamafuji and Irie.⁸ We have also measured the anisotropy of the pinning by varying the direction of J in the plane of the foil and find the above conclusions to apply for all angles. Thus the tensor form of (2) is probably correct as well. The observed anisotropy does not agree with any known model for anisotropic pinning; we expect to report on this in detail subsequently. We do conclude now that the early, simplest suggestions by Kim and Ander-

son⁹ are borne out in our case: The pinning force corresponds to a gradient in the fluxon self-energy (given by the tangent of the grating blaze angle in our case). Also, in our "one-dimensional" case, the size and spacing of the grooves enter Eq. (1) in a way that suggests that the pinning force density is simply proportional to the number of fluxons pinned.

We observe that while α_c is very reproducible, it is asymmetric with regard to current or field reversal. From Fig. 1(c) it is apparent that the static pinning force determined by the blaze angle will in fact not reverse its sense when the flux flow is reversed, so that the static pinning changes from "repulsive" to attractive, or vice versa. The asymmetry of α_c therefore implies that attractive and repulsive pinning are not of equal efficacy, again contradicting the suggestion that $f_p(\text{dynamic}) \propto f_p^2(\text{static})$.⁸ Although this rectification effect was unexpected, it may be similar to that observed by Swartz and Hart¹ who observed the effect, however, mainly when H was not normal to the surface.

Finally, we do observe the $J_c(H)$ peak, but only for foils imprinted by gratings with 100 and 140 grooves/mm spacings. The widths w of the grooves in the imprinted foils which exhibited the peak were always of the order of 15ξ , confirming a previous suggestion that the occurrence of the peak is a function mainly of the size or spacing of the pinners.¹⁰ Jones and Rose have noted that the J_c peak in Nb-O solutions and various other alloys occurs when second-phase particles exceed ξ by at least an order of magnitude.¹⁰ The removal of the J_c peak by copper plating on one side only (see above) may now be simply explained, since removal or alteration of pinning on that side changes the effective pinner spacing for the foil.

We gratefully acknowledge the support of the National Science Foundation; the aid and encouragement of Dr. L. A. Shepard, the technical help of I. M. Puffer, and the generosity of D. Schmitt of the Jarrell-Ash Company in providing us with the many gratings without which this work would not have been possible; also, the Allegheny-Ludlum fellowship which supported one of us (D.D.M.) for one part of the duration of this research.

*Work supported by the National Science Foundation.

¹P. S. Swartz and H. R. Hart, Jr., Phys. Rev. **137**, 818 (1965).

²D. G. Schweitzer and M. Garber, Phys. Rev. **160**,

348 (1967).

³W. C. H. Joiner and G. E. Kuhl, Phys. Rev. 163, 362 (1967).⁴H. J. Fink and W. C. H. Joiner, Phys. Rev. Lett. 23, 120 (1969).⁵J. D. Livingston, BNL Report No. 50155 (C-55), 1969 (unpublished).⁶D. C. Hill, J. G. Kohr, and R. M. Rose, Phys. Rev.Lett. 23, 764 (1969).⁷W. C. H. Joiner and G. E. Kuhl, Phys. Rev. 168, 413 (1968).⁸K. Yamafuji and F. Irie, Phys. Lett. 25A, 387 (1967).⁹P. W. Anderson and Y. B. Kim, Rev. Mod. Phys. 36, 39 (1964).¹⁰K. A. Jones and R. M. Rose, Phys. Lett. 27A, 412 (1968).

EFFECTS OF THE NÉEL TRANSITION ON THE THERMAL AND ELECTRICAL RESISTIVITIES OF Cr AND Cr:Mo ALLOYS

G. T. Meaden, K. V. Rao, and K. T. Tee

Department of Physics, Dalhousie University, Halifax, Nova Scotia, Canada

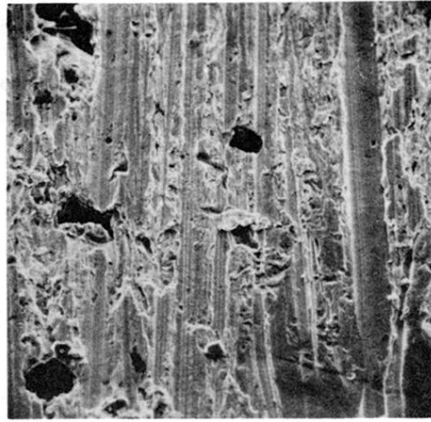
(Received 18 May 1970)

Thermal conductivity enhancements due to magnetic phase transitions have been observed for chromium, chromium-molybdenum alloys, and several rare-earth metals. The phenomenon can thus no longer be considered an uncommon one in metallic systems. In chromium, it appears to be sensitive to the microscopic state of particular samples.

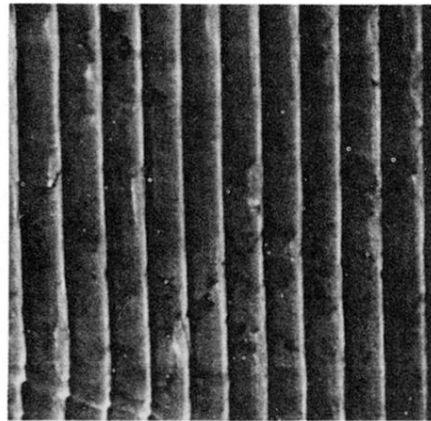
In a previous Letter¹ we presented evidence for an enhancement of the thermal conductivity of chromium in the vicinity of its Néel point T_N . It was suggested that the thermal-conductivity increase and corresponding Lorenz-number increase were related to the growth of critical fluctuations of the energy density of the spin-density-wave system. Because chromium is antiferromagnetic there also occurs magnetic superzone boundary scattering, and this is primarily responsible for the characteristic hump-backed part of the electrical resistivity curve below T_N . When the superzone resistivity is combined with the phonon and fluctuation resistivity contributions, there results a resistivity minimum close to T_N . A study of the experimental results led us to consider that superzone boundary scattering affects the thermal resistivity, too. This work has now been extended by investigating the temperature dependence of the thermal and electrical conductivities of dilute chromium alloys. The homologous element molybdenum was deemed a suitable solute because its presence is known to lower T_N and to raise rapidly the electrical resistivity in the antiferromagnetic state.² At the same time we wished to study the lattice contribution to the thermal conductivity and also to resolve the effects of band structure on the electronic contribution. A detailed discussion of these latter problems will be published elsewhere. The present results on chromium alloys have facilitated, for both the thermal and electrical resistivities, separation of the critical scattering

from other scattering effects, and have permitted independent substantiation of the results of the previous Letter on chromium. In addition, the original chromium sample has been well annealed and remeasured, and the new data confirm the correctness of the earlier work for the sample investigated. Since we have also observed thermal-conductivity enhancements at magnetic critical points in terbium and holmium single crystals³ and others have reported thermal-conductivity or Lorenz-number peaks at magnetic critical points in other rare-earth metals,⁴⁻⁷ we conclude that the effects reported in the present Letter for chromium and its alloys have a wider generality than hitherto supposed. We should also say that besides the intrinsic importance of the new results reported herein, they are also of significance in view of two other recent Letters to this journal.^{8,9} These references will be referred to as MWM and LM, respectively.

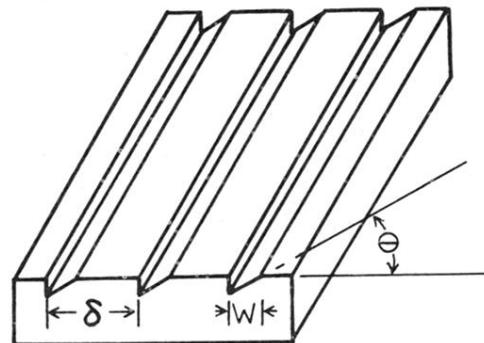
Our method for determining the thermal conductivity $\lambda(T)$ was, as before, that of longitudinal heat flow using Au-0.03 at. % Fe against chromel-P for the differential thermocouple thermometry. Probe separation for the various samples was 3 to 4 cm and the temperature differences lay in the range 0.2 to 0.3°K over this length. The output from this differential thermocouple was detected by a Honeywell centimicrovolt potentiometer, type 2779, in conjunction with a Guildline galvanometer-amplifier system. This permitted a voltage drift of 1 nV during the course of an hour to be discerned. Prior to our first chromi-



A



B



C

FIG. 1. (a) The surface of In-2% Bi foil abraded with No. 600 paper (scanning electron microscope, 490 \times). (b) In-2% Bi foil imprinted with diffraction grating, 590 lines/mm. (Scanning electron microscope, 5000 \times ; for the measurement of groove width, 20 000 \times was used when necessary.) (c) Schematic of imprinted surface, showing groove width w , blaze angle θ , and groove spacing δ .